# Motion Associated with a Single Rouse Segment versus the α Relaxation. 2

**Y.-H. Lin***

*Department of Applied Chemistry, National Chiao Tung University, Hsinchu, Taiwan*

*Received: August 19, 2004; In Final Form: May 27, 2005*

The dynamics in polystyrene melt and concentrated solution as probed by depolarized photon-correlation spectroscopy has been shown to reflect the motion associated with a single Rouse segment. In the concentrated solution case (entanglement-free), the analysis using the frictional factor $K$ ($=\zeta\langle b^2\rangle/kT\pi^2m^2$) extracted from the viscosity data in terms of the Rouse theory and aided by the Monte Carlo simulation based on the Langevin equation of the Rouse model confirms the conclusion in a precise manner. In the melt case (entangled), the Rouse-segmental motion as observed by depolarized photon-correlation spectroscopy is compared with the α relaxation and the highest Rouse−Mooney normal mode extracted from analyzing the creep compliance $J(t)$ of sample A reported in the companion paper. Another well-justified way of defining the structural (α-) relaxation time is shown basically to be physically equivalent to the one used previously. On the basis of the analysis, an optimum choice $\tau_S = 18\langle\tau\rangle_G$ ($\langle\tau\rangle_G$ being the average glassy-relaxation time) is made, reflecting both the temperature dependence of $\langle\tau\rangle_G$ and the effect on the bulk mechanical property by the glassy-relaxation process. In terms of thus defined $\tau_S$, two traditional ways of defining the α-relaxation time are compared and evaluated. It is shown that as the temperature approaches the calorimetric $T_g$, two *modes of temperature dependence* are followed by the dynamic quantities concerning this study: One includes the time constant of the highest Rouse−Mooney normal mode, $\tau_v$; the temperature dependence of the viscosity corrected for the changes in density and temperature, $\eta/\rho T$; and the average correlation time obtained by depolarized photon-correlation spectroscopy, $\langle\tau_c\rangle$. The other, being steeper, is followed by the α-relaxation time $\tau_S$ derived from the glassy-relaxation process and the temperature dependence of the recoverable compliance $J_r(t)$ as obtained by Plazek. The comparison of the dynamic quantities clearly differentiates the motion associated with a single Rouse segment as characterized by $\tau_v$ or $\langle\tau_c\rangle$ from the α-relaxation as characterized by $\tau_S$; due to the lack of clear definition of these two types of motion in the past and the proximity of one to the other in the time scale—actually the two crossing over each other—as the temperature is approaching $T_g$, the two modes could be easily confused. Below ∼110 °C, the rate of $\langle\tau_c\rangle$ changing with temperature lags behind that of $\tau_v$ is explained as due to the loss of effective ergodicity taking place in the system.

## 1. Introduction

The Rouse model[1] is based on picturing a polymer chain as a linkage of beads and springs.[2−4] Each bead−spring segment is often referred to as the Rouse segment. The distribution of the separation between two neighboring beads is described by a Gaussian function. The motion associated with a single Rouse segment is basically equivalent to the highest Rouse normal mode of motion in a polymer chain. If the polymer chain is very long, and we are interested in only the few slowest modes of chain motion—for instance, as mainly reflected by the zero-shear viscosity—the length of chain section assigned to a Rouse segment is not an issue as long as the chosen section is much smaller than the whole chain and at the same time sufficiently long. However, the highest Rouse mode becomes relevant, and how to define a Rouse segment becomes a concern, if we are interested in the relatively fast $T_g$-related α-relaxation that shows up in the high-modulus region of a typical viscoelastic spectrum as the temperature is lowered toward $T_g$.[5−12] An ideal Rouse segment cannot be found in reality, as the Gaussian function allows the spring between two beads to be stretched infinitely—a situation that cannot occur because of the rigidity of chemical bonds. Thus, if a Rouse segment can be defined experimentally, it has to be probed in the linear region, for instance, by measurements of linear viscoelasticity and photon-correlation function. Furthermore, the Rouse segment as expected to be seen here is not a clear geometric identity but rather is represented by an optimum size or mass that, for instance in an entanglement-free case, allows the experimental results to be best described in terms of the *discrete* Rouse model for a chain with a *finite* number of beads.[3,4] In this paper, the theoretical aspect of relating the depolarized photon correlation to viscoelasticiy in a concentrated polystyrene system will first be reviewed. Then, three related points will be addressed: (1) The dynamics in polystyrene melt and concentrated solution as probed by depolarized photon-correlation spectroscopy has been shown to reflect the motion associated with a single Rouse segment as expected from the theoretical analysis. In particular, it will be illustrated how this is shown in a precise manner in the entanglement-free concentrated solution case. The Rouse-segmental motion in melt (entangled) as observed this way will be compared with the α-relaxation and the highest Rouse−Mooney normal mode extracted from analyzing the creep compliance $J(t)$ of sample A reported in the preceding paper (ref 11)—the results of sample B cannot be used here because of its contamination by residual plasticizers. (2) In this paper, another well-justified definition of the structural (α-) relaxation

* E-mail: yhlin@mail.nctu.edu.tw.

10.1021/jp040567s CCC: $30.25 
Published on Web 08/24/2005

**TABLE 1: Values of $K$, $s$, $\tau_v$, $\langle\tau\rangle_G$, $t_m$, and $\tau_S$ of Sample A ($M_w = 4.69 \times 10^4$) at Different Temperatures[a]**

| $t$ (°C) | $K$ | $s$ | $\tau_v$ | $\langle\tau\rangle_G$ | $t_m$ | $\tau_S$ |
|---|---|---|---|---|---|---|
| 127.5 | $4.8 \times 10^{-9}$ | | $2.28 \times 10^{-3}$ | | | |
| 125 | $9.08 \times 10^{-9}$ | | $4.3 \times 10^{-3}$ | | | |
| 114.5 | $1.96 \times 10^{-7}$ | 6 283 | $9.3 \times 10^{-2}$ | $1.23 \times 10^{-3}$ | $1.78 \times 10^{-2}$ | $2.21 \times 10^{-2}$ |
| 109.6 | $1.2 \times 10^{-6}$ | 10 053 | 0.569 | $1.21 \times 10^{-2}$ | 0.186 | 0.218 |
| 104.5 | $1.2 \times 10^{-5}$ | 16 337 | 5.69 | 0.196 | 3.39 | 3.53 |
| 100.6 | $9.7 \times 10^{-5}$ | 28 275 | 46 | 2.74 | 56.2 | 49.4 |
| 97 | $9.84 \times 10^{-4}$ | 56 550 | 467 | 55.6 | 1349 | 1002 |

[a] All relaxation times are in unit of s.

time is shown basically to be physically equivalent to the one used previously.[11] For reflecting both the temperature dependence of the glassy-relaxation process accurately and the effect on the bulk mechanical property, an optimum choice $\tau_S = 18\text{-}\langle\tau\rangle_G$ is made. In terms of thus defined $\tau_S$, two traditional ways of defining the α-relaxation time[5] are compared and evaluated. (3) A distinction between the Rouse-segmental motion as studied by the depolarized photon-correlation spectroscopy and the α-relaxation should be made. Due to the lack of clear definition of these two types of motion in the past and the proximity of one to the other in the time scale, the mode of motion that should have been considered as the Rouse-segmental motion could be confused with the α-relaxation.[13] Finally, various dynamic quantities obtained from analyzing the depolarized photon-correlation and creep compliance results are compared and discussed.

## 2. Summary of Molecular Theories of Polymer Viscoelasticity

Successful molecular theories of polymer viscoelasticity in the entanglement-free region, the Rouse model,[4,14,15]and in the entanglement region, the extended reptation model,[4,16,17,18,19] have been developed using the Rouse segment as the most basic—smallest—structural unit. These theories are mean-field theories; the bulk viscoelastic quantity is simply the sum of the average values from individual model molecules.[2−4] The friction constant $\zeta$ associated with each Rouse segment or equivalently the frictional factor $K$ as defined below is a basic element of such a mean field:[4,11,14−19]

$$K = \frac{\zeta\langle b^2\rangle}{kT\pi^2 m^2} \tag{1}$$

where $m$ and $b$ are the mass and length of a Rouse segment, respectively. $K$ alone carries the temperature dependence of the Rouse segment-based relaxation times, which often follows the Fulcher and Tammannn−Hesse (FTH) equation or the Williams−Landel−Ferry (WLF) equation.[5] The extended reptation theory (ERT)[4,16] is developed by incorporating the intramolecular Rouse-type motions into the Doi−Edwards theory.[20] In addition to the use of the Rouse segment, ERT contains the basic mean-field assumption of the Doi−Edwards theory (i.e., the definition of the primitive chain as represented by the following equation):

$$N\left(=\frac{M}{M_e}=\frac{N_o}{N_e}\right)=\frac{L}{a}=\frac{\langle R^2\rangle}{a^2}=\frac{N_o\langle b^2\rangle}{a^2} \tag{2}$$

where $L$ denotes the contour length of the primitive chain, $a$ is the distance between two ends of an entanglement strand with mass $M_e$ or equivalently $N_e$ ($= M_e/m$) Rouse segments, and $\langle R^2\rangle$ represents the mean square end-to-end distance of a polymer chain with mass $M$ or equivalently $N_o$ ($= M/m$) Rouse segments. The frictional factor $K$ in ERT is shown to be independent of molecular weight to as low as just above the entanglement molecular weight $M_e$ (see Appendix B and Table 1 of ref 11), proving the validity of ERT.[4,14−19] The validity of the Rouse theory[4,14,15] as well as its consistency with ERT by sharing the same frictional factor $K$[4,18] has been extensively tested by experimental results. It is an important contribution of ERT to bridge the gap between the Rouse and Doi−Edwards theories by showing that they have the same footing at the Rouse-segmental level. Because of this result, the frictional factor $K$ extracted from the viscoelastic results in terms of either the Rouse theory or ERT can be used in the same way in comparing with the depolarized photon-correlation results, as done previously[9,10,21−23] and in this study.

For both the studies of the motion associated with a single Rouse segment and the α-relaxation, the strategy we take is to use the successful description of the slow (low-frequency) viscoelastic properties—for instance, the zero-shear viscosity and the viscoelastic spectrum from the low-frequency end of the transition zone to the terminal zone—in terms of the molecular theories as the reference frame.[9−11,21−23] The molecular theory used for analyzing the experimental results depends on whether the system is in the entanglement or entanglement-free region. Then, the frictional factor $K$ thus determined can be used to calculate the time constant of the highest Rouse normal mode for comparison with other dynamic results or be used to "normalize" the α-relaxation time for further comparative analysis.

In the Rouse model, the relaxation modulus $G(t)$ for a monodisperse polymer of molecular weight $M$ or $N_r$ beads is obtained as[1,3,4]

$$G(t) = \left(\frac{\rho RT}{M}\right)\mu_R(t/\tau_R) \tag{3}$$

with

$$\mu_R(t/\tau_R) = \sum_{p=1}^{N_r-1}\exp\left(\frac{-t}{\tau_R^p}\right) \tag{4}$$

where $\rho$ is the concentration of the polymer (mass per unit volume) and $\{\tau_R^p\}$ is given by

$$\tau_R^p = \frac{\zeta\langle b^2\rangle}{24kT\sin^2\left(\frac{p\pi}{2N_r}\right)} = \frac{K\pi^2M^2}{24N_r^2\sin^2\left(\frac{p\pi}{2N_r}\right)} \qquad p = 1, 2, ..., N_r - 1 \tag{5}$$

For $N_r \gg 1$, the zero-shear viscosity may be obtained from $G(t)$ as

$$\eta = \int_0^\infty G(t)\,dt = K\left(\frac{\rho RT\pi^2}{36}\right)M \tag{6}$$

If the molecular weight of a Rouse segment ($m$) is known, the relaxation time of the highest Rouse viscoelastic normal mode ($\tau_v$) can be calculated according to

$$\tau_v = \frac{K\pi^2 m^2}{24} \tag{7}$$

which is obtained by substituting $p = N_r - 1$ into eq 5 and taking $(N_r - 1)/N_r \approx 1$ for $N_r$ sufficiently large. The frictional factor in eq 7 can be obtained from the viscosity data analyzed in terms of eq 6. Thus, from the viscosity measurement, the information of the Rouse-segmental motion characterized by $\tau_v$ can be obtained. In this paper, all the relaxation times are given in the unit of seconds, and the molecular masses: $M$, $M_e$, and $m$, are in the unit of Daltons. Thus, $K$ has the unit of s/Da$^2$.

A summary of ERT has been given in the companion paper[11] (eqs 1 and 2). The relaxation times of the $\mu_A(t)$, $\mu_X(t)$, $\mu_B(t)$, and $\mu_C(t)$ processes are each expressed as a product of the frictional factor $K$ (denoted by $K'$ for $\mu_A(t)$) and a structural factor. Except for the $\mu_A(t)$ process, we refer all the functional forms of the relaxation processes and their respective characteristic (relaxation) times to previous publications.[4,16−18] As first shown by Mooney,[4,16,24,25] $\mu_A(t/\tau_A)$ and $\tau_A^p$ have the same forms as $\mu_R(t/\tau_R)$ and $\tau_R^p$ (eqs 4 and 5), respectively, with $M$ replaced by $M_e$ and $N_r$ replaced by $N_e$. In applying the equation for $\tau_A^p$, the frictional factor $K$ needs to be replaced by $K'$ as given by eq 8 of ref 11.

### 3. Rouse-Segmental Motion as Probed by Depolarized Photon-Correlation Spectroscopy

The usual mode of photon-correlation spectroscopy—self-beating—is based on the condition that the scattered light field obeys Gaussian statistics.[26,27] This makes it particularly suitable and popular for probing dynamics in systems "populated" by Brownian particles as exemplified by the numerous studies of polymer chain dynamics in solutions.[27,28] Depolarized dynamic light scattering being much affected by the fast fluctuations of polarizability anisotropy, it is expected that depolarized photon-correlation spectroscopy mainly probes the reorientation motion of a correlated region.[29] Since the Rouse segment is the most basic Brownian particle in the Rouse model, which describes very well the polymer viscoelastic behavior over at least the intermediate- and long-time regions of an entanglement-free concentrated system,[4,14,15] the depolarized photon-correlation function may provide the information about the motion of a single Rouse segment. Such an expectation is borne out by recent studies[9,10,21−23] as summarized below:

Depolarized photon-correlation spectroscopy was first used to study the chain dynamics in a well-entangled polystyrene melt by Patterson et al.[13] It was later pointed out by Lin[9,10] that the average correlation time $\langle\tau_c\rangle$ obtained by Patterson follows the same temperature dependence as that of viscosity of nearly monodisperse polystyrene samples obtained by Plazek and O'Rourke[30] from 130 to 110 °C (see Figure 5; the correction for the changes in density and temperature as made in the figure causes only a negligible difference). The $\langle\tau_c\rangle$ value changing by a factor as large as 356 over this temperature range, the agreement is significant, suggesting strongly that the observed time constant is basically $\tau_v$ (i.e., of the same order of magnitude) as given by eq 7, which shares the same frictional factor $K$ as that of viscosity (eq 6).

$K$ of polystyrene at 127.5 °C is given by the average value listed in Table 1 of ref 11 to be $5.2 \times 10^{-9} \pm 10\%$. The structural factors of the relaxation times of the Rouse−Mooney normal modes $\{\tau_A^p\}$ are independent of molecular weight. At the same time, if the molecular weight is sufficiently high, $K'/K$ is at the plateau value 3.3 based on eq 8 of ref 11. The polystyrene sample studied by Patterson et al. was prepared by thermal polymerization at 90 °C. Under such a condition, its number-average molecular weight is expected to be around 400 000;[31] in other words, it is in the highly entangled region where the plateau value of $K'/K$ is applicable, even though its molecular weight distribution is not nearly monodisperse. Thus, we can use the above $K$ value at 127.5 °C and the ratio $K'/K = 3.3$ to obtain $K'$. As explained in ref 11, the mass of a Rouse segment of polystyrene ($m$) being about 850[6−12,21−23,32,33] leads to $N_e = 16$. Using the value of $K'$ obtained as described above and $N_e = 16$ or equivalently $m = 850$, we can calculate $\tau_v \approx \tau_A^{15}$ from eq 7 or eq 5 (with $K$ substituted by $K'$; and $N_r$ replaced by $N_e = 16$) to be $5.1 \times 10^{-3}$ sec, which, clearly as expected, is of the same order of magnitude as the $\langle\tau_c\rangle$ value at 127.5 °C, $3.5 \times 10^{-3}$, obtained from Patterson's results by interpolation.

In the case of polystyrene, it has been shown that the effective optical anisotropy per monomer unit from polystyrene in melt and in solution (cyclohexane as the solvent, whose depolarized light scattering is negligible) is the same,[34,35] indicating that the static correlation between segments belonging to *different* chains is nil. And the dynamic pair correlation is in general much smaller than the static pair correlation.[29,36] On the basis of neglecting both the static and dynamic pair correlation among segments belonging to different chains and assuming that the size of the polymer coil is much smaller than the scattering wavelength and that the collective reorientation time is much shorter than the time needed for the center-of-mass of the polymer chain to travel the distance of a scattering wavelength, the time-correlation function for depolarized Rayleigh light scattering can be expressed as[9,10,21−23]

$$C(t) = [Sf_s(t) + R]\langle P_2[\mathbf{u}(t)\cdot\mathbf{u}(0)]\rangle \tag{8}$$

where $P_2$ is the second-order Legendre polynomial; $\mathbf{u}(t)$ is the unit vector representing the direction of the symmetry axis of a correlated region—the whole region is regarded as a Kuhn segment or equivalently a Rouse segment [37]—along the polymer chain at time $t$; $f_s(t)$ is a normalized time-correlation function that reflects the motions associated with the local chemical bonds, which are grossly referred to as the sub-Rouse-segmental motion; the relaxation strength $S$ depends on the details of bond angles and steric interactions among chemical bonds; and $R$ is a constant that is related to how anisotropic the correlated region is.

The depolarized photon-correlation functions of two entanglement-free concentrated solutions (∼60 wt %) of polystyrene with $M_w = 9100$; $M_w/M_n = 1.02$, and $M_w = 18\,100$; $M_w/M_n = 1.01$ in cyclohexane at the $\theta$ condition (i.e., at 35 °C)—denoted by samples S1 (59.832 wt %; 0.552 g/cm$^3$) and S2 (60.287 wt %; 0.556 g/cm$^3$), respectively—have been measured and analyzed.[21−23] Along with the depolarized photon-correlation measurements, two solution samples with accurately determined concentrations in the close neighborhood of the concentration of each of the two samples, S1 and S2, are prepared for viscosity measurements by the falling-ball method, which, with both the ball and solution sealed in a glass tube, is particularly good for studying solution systems as solvent evaporation can be prevented. Then, by interpolation or extrapolation, the viscosity values at the concentrations of samples S1 and S2 can be individually determined; subsequently, their $\tau_v$ values can be calculated (eqs 6 and 7) for comparison with their depolarized photon-correlation results. Furthermore, the obtained information

of the concentration dependence of viscosity allows the viscosity results to be compared under the same concentration and can be used to correct for the small concentration difference between samples S1 and S2 when their depolarized photon-correlation results are compared. The discussions below are all based on the results after the corrections have been made; the details of the corrections can be found in ref 21.

The obtained molecular weight dependence of viscosity at the same concentration (60 wt %) indicates that the Rouse theory is applicable; in other words, the concentrations of the studied polystyrene solutions are high enough to screen out the hydrodynamic interactions.[2] This conclusion is further confirmed by analyses in terms of the Rouse theory in other aspects of experiments as will be described below. Through the multiexponential singular value decomposition (MSVD) analysis,[27] a bimodal relaxation-time distribution can clearly be obtained from the depolarized photon-correlation functions of both S1 and S2, as corresponding to the two modes of motion in eq 8. Because of the limitation of the time window of photon-correlation spectroscopy, only the tail region of the fast mode $f_s(t)$ can be observed. Thus, as far as the fast mode is concerned, one can only show its existence from the MSVD analysis. However, much information about the slow mode $\langle P_2[\mathbf{u}(t)\cdot\mathbf{u}(0)]\rangle$ has been obtained from the analysis of the experimental results.[21−23] It has been shown that the slow mode, with a rather narrow relaxation-time distribution—extending over slightly less than two decades, is *independent of scattering angle and molecular weight* in accordance with eq 8. In the polystyrene melt case, the depolarized photon-correlation function is well-described by the stretched exponential form with the stretching exponent $\beta$ near 0.4. This corresponds to a unimodal broad relaxation-time distribution, covering more than five decades.[38] The fact that the two modes of motion as contained in eq 8 cannot be separated in melt as in the concentrated-solution case is explained as due to the stronger interactions among segments causing the two modes to overlap extensively.

Assuming $\mathbf{u}(t) = \mathbf{b}(t)/|\mathbf{b}(t)|$, the time-correlation function $\langle P_2[\mathbf{u}(t)\cdot\mathbf{u}(0)]\rangle$ can be calculated by the Monte Carlo simulation based on the Langevin equation of the Rouse model.[4,22] Also, from the simulation, the ratio between $\tau_v$ (corresponding to eq 7) and the average correlation time $\langle\tau\rangle_r$ obtained from integrating the simulated $\langle P_2[\mathbf{u}(t)\cdot\mathbf{u}(0)]\rangle$ curve can be calculated for comparison with the experimental results $\langle\tau\rangle_2/\tau_v$ ($\langle\tau\rangle_2$ denotes the average correlation time of the slow mode obtained from resolving the measured photon-correlation function, while $\tau_v$ is calculated from the viscosity data through eqs 6 and 7). In comparing the analyses of the depolarized photon-correlation function, viscosity, and Monte Carlo simulation results, we have found that $m = 1130$ gives a good overall agreement: Corresponding to $m = 1130$, $N_r = 8$ and 16 for samples S1 and S2, respectively. From the results of the depolarized photon-correlation function and viscosity, we obtained $\langle\tau\rangle_2/\tau_v = 2.4$ and 2.6 for samples S1 and S2, respectively; from the simulation, we obtained $\langle\tau\rangle_r/\tau_v = 2.2$ and 2.5 for $N_r = 8$ and 16, respectively. Furthermore, as shown in Figure 1, the line shapes of the time-correlation functions of the slow mode of both samples S1 and S2 (denoted by $\langle C_2(t)\rangle$) are in close agreement with the simulation results of $\langle P_2[\mathbf{u}(t)\cdot\mathbf{u}(0)]\rangle$ for $N_r = 8$ and 16. Thus, despite the crudeness of the Rouse segment, the effect of chain connectivity as contained in the Rouse model can quite fully account for the detailed aspect of the dynamics as showing up in the depolarized photon-correlation function and its relation with viscosity, supporting the physical picture that the dynamic process probed by depolarized photon-correlation spectroscopy

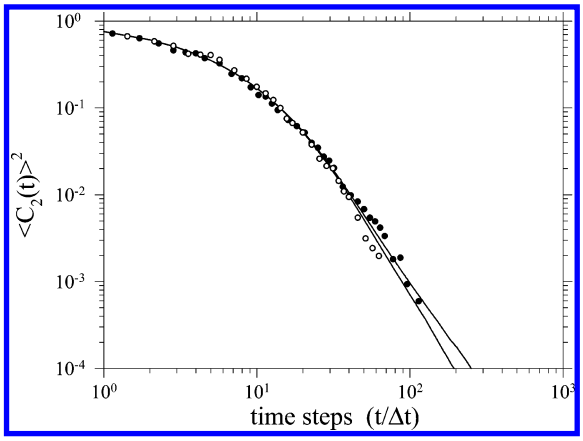


**Figure 1.** Comparison of the $\langle P_2[\mathbf{u}(0)\cdot\mathbf{u}(t)]\rangle^2$ dynamic processes obtained from the depolarized photon-correlation functions of the S1 (○) and S2 (●) samples and the simulation results of the Rouse chain with $N_r = 8$ (the left solid line) and with $N_r = 16$ (the right solid line).

is the reorientation motion of a Rouse segment. The mass of a Rouse segment obtained for the studied concentrated polystyrene solutions, $m = 1130$, is about 25% larger than that in the melt. This small difference should be due to the presence of solvent; indeed, the small solvent-enhancement effect is about that expected from the concentration dependence of the Rouse segment size obtained by Inoue et al.[12] from analyzing the dynamic mechanical and birefringence results—the expected $m$ value at the studied concentration is about 1100 versus 850 in the melt (see Figure 10 of ref 12). The agreement between the two independent studies based on very different premises[39] reconfirms that the Rouse segment size can be defined and that the motion associated with a single Rouse segment can indeed be studied; in other words, the study of the Rouse-segmental motion as presented above is well supported.

In summing up the above studies of polystyrene melt and concentrated solutions, we can notice differences and common points: The differences between the melt case and the concentrated solution case are mainly two: (1) The relaxation-time distribution is much broader in the former than in the latter and (2) the $\langle\tau_c\rangle/\tau_v$ ratio is smaller in the former than in the latter (denoted by $\langle\tau\rangle_2/\tau_v$ in the latter case). These two differences can be accounted for by the stronger interactions among segments in the melt—in the concentrated solution case, the interactions among segments can be much reduced by the "lubrication" of the solvent molecules. Due to the stronger interactions in the melt case, the fast and slow modes as contained in eq 8 overlap extensively; the photon-correlation function cannot be resolved into the two modes. While the effect leads to a broad unimodal relaxation-time distribution,[13,38] the fast component in the distribution also causes the observed average relaxation time $\langle\tau_c\rangle$ to be smaller than when only the slow component contributes to it as in the concentrated solution case. The main shared common point is the applicability of the Rouse model—either as $\mu_R(t/\tau_R)$ or as $\mu_A(t/\tau_A)$, which is a part of ERT—in relating the viscoelasticity results to the dynamics observed by depolarized photon-correlation spectroscopy. As the melt system and the concentrated solution system at the $\theta$ point are very similar dynamically and thermodynamically—both free of the hydrodynamic interactions and excluded-volume effect[2]—the precise analysis achieved in the concentrated solution case lends additional support to the analysis of the melt results, in which some of the details are prevented by the much broader relaxation-time distribution in $C(t)$ from being revealed.

In summary, the recent studies as briefly described above confirm the initial expectation that the motion of a single Rouse

segment can be studied by depolarized photon-correlation spectroscopy. This conclusion has a bearing on the comparison of the α-relaxation with the highest Rouse−Mooney normal mode, both extracted from the creep compliance $J(t)$ as reported in ref 11.

#### 4. α-Relaxation in Creep Compliance

With $G(t)$ known—for instance as given by eqs 1, 4, and 5 of ref 11—$J(t)$ can be calculated numerically by the method of Hopkins and Hamming.[40,41] It has been shown in detail in ref 11 that the rubber(like)-to-fluid region of Plazek's $J(t)$ results of two nearly monodisperse polystyrene samples[42,43] can be well-described by ERT and that the dynamic information of the glassy-relaxation process as contained in the small-compliance/short-time region of $J(t)$ can be meaningfully extracted by using the successful description of the rubber(like)-to-fluid region in terms of ERT as the reference frame. The glassy-relaxation process is found to be well described by the stretched exponential form

$$A_G\mu_G(t/\tau_G) = A_G \exp\left[-\left(\frac{t}{\tau_G}\right)^{\beta}\right] \tag{9}$$

as incorporated into eq 4 of ref 11. In the whole relaxation-time distribution, the glassy-relaxation region is situated in a certain position relative to the rubber(like)-to-fluid region, where all the relaxation times are proportional to the frictional factor $K$. The relative position has been expressed by

$$\langle\tau\rangle_G = sK \tag{10}$$

where $s$ is a proportional constant and has the unit of Dalton square. The parameter $s$ represents the glassy-relaxation time with $K$ fixed at 1 or any constant; it is regarded as a normalized glassy-relaxation time. In the vicinity of $T_g$, the parameter $s$ increases with decreasing temperature, reflecting the thermorheological complexity between the glassy-relaxation process, $A_G\mu_G(t)$, and the ERT processes: $\mu_A(t)$, $\mu_X(t)$, $\mu_B(t)$, and $\mu_C(t)$, in the rubber-to-fluid region and indicating the existence of a structural length scale as discussed in detail in ref 11.

Sample B whose $J(t)$ results were analyzed in ref 11 is contaminated by residual plasticizers; the $K$ value extracted from it cannot be used for comparing with studies on normal (uncontaminated) samples. Thus, in this report, we only discuss the results of sample A. It has been found for sample A that $A_G$ (= 5482) and the stretching parameter $\beta$ (= 0.41) are very much independent of temperature, while $s$ increases with decreasing temperature significantly—by about an order of magnitude over the covered temperature range. The obtained $K$ and $s$ values at different temperatures for sample A are listed in Table 1. Using the obtained $K$ and $s$ values in the $\tau_A^p$ equation (i.e. eq 5 with $K$ replaced by $K' = 1.61K$ as calculated from eq 8 of ref 11 for $M = 4.69 \times 10^4$; $M$ replaced by $M_e$; and $N_r$ replaced by $N_e = 16$) and eq 10, the $\tau_v \approx \tau_A^{15}$ and $\langle\tau\rangle_G$ values at different temperatures can be, respectively, calculated as also shown in Table 1.

One may calculate the $J(t)$ curves at different temperatures *in real time* with the $K$ and $s$ values shown in Table 1. Instead of doing this way, the comparisons of the $J(t)$ curves of sample A measured at different temperatures to those calculated with $K$ fixed at $5 \times 10^{-9}$ and the $s$ values listed in Table 1 are shown in Figure 1 of ref 11. This illustrates using the description of the rubber(like)-to-fluid region of $J(t)$ in terms of ERT as the reference frame to show the effect of temperature on the glassy-relaxation process; such a comparison serves the purpose of reflecting and characterizing in perspective the thermorheological complexity occurring in $J(t)$ as the temperature is near $T_g$. As also shown in ref 11, unlike the extensive overlapping of the different processes in $J(t)$, the individual processes can be clearly shown in the $G(t)$ form. Based on the obtained $G(t)$ results, a structural relaxation time $\tau_S$ was defined as the time when $G/R$ has declined to 3 as described in detail in ref 11. The thus defined structural relaxation time becomes greater than $\tau_v$ just before the temperature reaches $T_g$, indicating vitrification at the Rouse-segmental level.

As will be shown below, the structural relaxation time defined by $G/R = 3$ can be considered as basically equivalent to the so-called α-relaxation time. In the literature, the α-relaxation time has been "defined" in different ways,[5,44] such as the reciprocal of the frequency at the peak of tan $\delta$ and the reciprocal of the frequency at which the storage modulus $G'(\omega)$ is at $10^8$ dyn/cm$^2$. The relaxation time defined in any of these ways can in principle be determined clearly by experiment. However, it does not really characterizes a relaxation process in a simple and clear manner; with a temperature change, it is affected not only by the intrinsic temperature dependence of the relaxation process that matters but also by the change in the line shape of the viscoelastic spectrum (namely, the thermorheological complexity). The structural relaxation time defined as the time when $G/R = 3$ has a similar defect.

To further illustrate the physical effect on the bulk mechanical property by the glassy relaxation, another analysis will be made below. This analysis confirms the basic physical uniqueness of $\tau_S$ as defined by the time when $G/R = 3$. On the basis of these findings, an optimum definition for $\tau_S$ is chosen, which has an unambiguous meaning in its temperature dependence and at the same time properly reflects the effect on the bulk property by the glassy relaxation. And it will be shown below that the thus defined $\tau_S$ is very close to the α-relaxation time defined by one of the traditional ways.

We consider that the time when the absolute value of the slope d(log $G(t)$)/d(log $t$), denoted by $H$, reaches its first maximum reflects a unique physical meaning associated with the glassy-relaxation process as explained in the following: As shown previously and mentioned above, the $\mu_G(t)$ process can be well-described by the stretched exponential form with $\beta = 0.41$, which is very much independent of temperature. In the high-modulus/short-time region where the glassy-relaxation process dominates

$$H = \left|\frac{\mathrm{d}(\log G(t))}{\mathrm{d}(\log t)}\right| = \beta\left(\frac{t}{\tau_G}\right)^{\beta} \tag{11}$$

As shown in Figure 2, initially following eq 11, log $H$ increases with log $t$ with a slope of $\beta = 0.41$, indicating a gradually steeper decline of log $G(t)$ with log $t$. At the time, denoted by $t_m$, when $H$ reaches its first maximum, while the *rate* of the glassy-relaxation process has the greatest influence, its modulus magnitude is losing its dominance as deviation from eq 11 begins taking place. As it turns out, the location of the $H$ maximum occurs in the neighborhood of the structural relaxation time defined as the time when $G/R = 3$. The obtained $t_m$ values at different temperatures are listed in Table 1, which occur in the range of 15−25 $\langle\tau\rangle_G$, depending on the temperature. The obtained $\langle\tau\rangle_G$ values occur in the too short-time region to clearly reflect the dynamic effect of the glassy-relaxation process on the bulk mechanical property; however, they carry the intrinsic temperature dependence of the glassy-relaxation process. To have the benefits of both $t_m$ and $\langle\tau\rangle_G$, we redefine the structural relaxation time arbitrarily as $\tau_S = 18\langle\tau\rangle_G$, whose values at different temperatures are also listed in Table 1. Allowing a

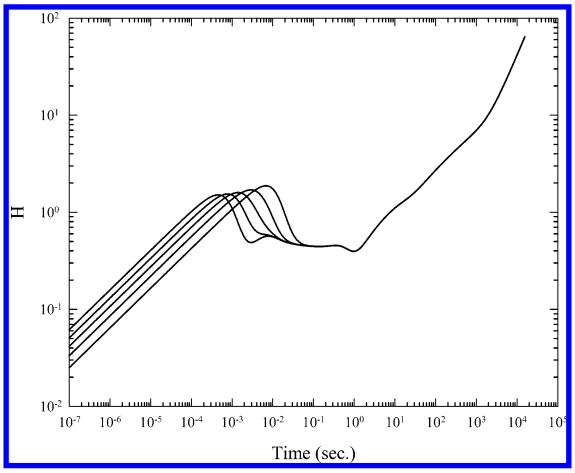


**Figure 2.** *H* indicating the declining rate of log $G(t)$ vs log $t$, as defined in the text, is shown as a function of time for sample A at 114.5, 109.6, 104.5, 100.6, and 97 °C corresponding to lines from left to right, respectively; all calculated with $K$ fixed at $5 \times 10^{-9}$ and the respective $s$ values listed in Table 1.

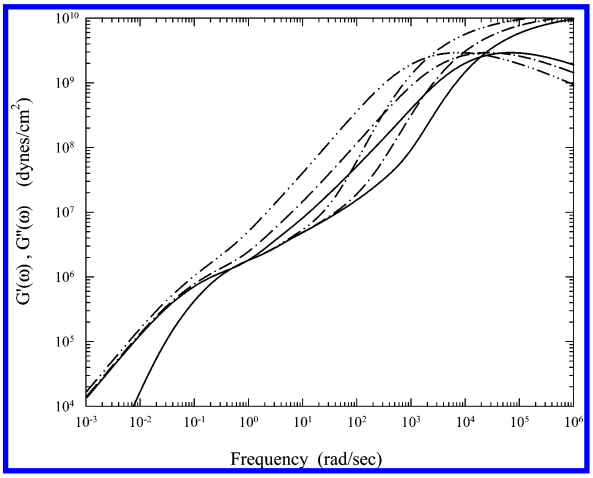


**Figure 3.** Comparison of the storage- and loss-modulus spectra, $G'(\omega)$ and $G''(\omega)$, of sample A at 114.5 (—), 104.5 (— · —), and 97 °C (— · · —) all calculated with $K$ fixed at $5 \times 10^{-9}$ and the respective $s$ values listed in Table 1.

20% deviation from this somewhat arbitrarily chosen $\tau_S$—for instance one may as well choose $\tau_S = 22\langle\tau\rangle_G$—the main point that will be explained in terms of the defined $\tau_S$ remains the same.

For comparing the above-defined $\tau_S$ with the α-relaxation time defined in the literature, the storage-, loss-modulus, and tan $\delta$ spectra of sample A are shown in Figures 3 and 4, all the spectra being "normalized" with respect to $K = 5 \times 10^{-9}$ (see the Appendix for the calculations of the spectra). As, being basically a mirror image, the $G'(\omega)$ spectrum has a close match to $G(t)$ if $\omega = 0.7/t$ is used in the conversion between time and frequency, we define $\omega_S = 0.7/\tau_S$.[45] The thus defined $\omega_S$ values at 114.5, 104.5, and 97 °C are compared in Figure 4 with what have been used traditionally: at the peak of tan $\delta$ and at $G'(\omega) = 10^8$ dyn/cm$^2$. It can be seen that the $\omega_S$ values at the three shown temperatures occur in the close neighborhood of the frequencies where the respective storage-modulus has the value $10^8$ dyn/cm$^2$; however, they deviate considerably from the respective frequencies at the tan $\delta$ maximum. In a case where a careful analysis as done in this study is not feasible, using $G'(\omega) = 10^8$ dyn/cm$^2$ as the criterion for deciding the α-relaxation time may be a good choice except bearing that the thus determined relaxation time does not follow exactly the temperature dependence of $\langle\tau\rangle_G$ as the above-defined $\tau_S$ does.

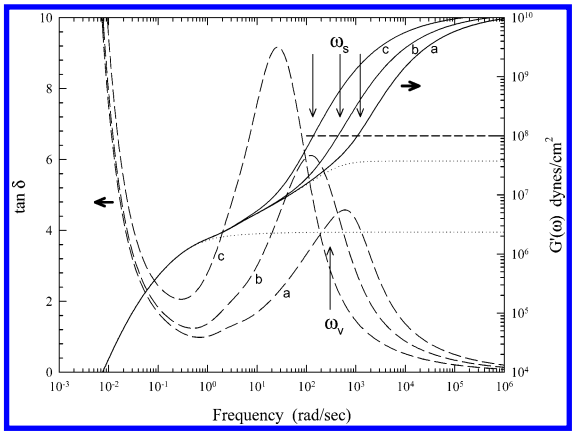


**Figure 4.** Comparison of the storage-modulus (—) and loss-tangent (- - ) spectra of sample corresponding to those shown in Figure 3: a, for 114.5 °C; b, for 104.5 °C; c, for 97 °C. Also shown are the $\omega_S = 0.7/\tau_S$ values (right ↓ for a; middle ↓ for b; left ↓ for c) calculated with $K$ fixed at $5 \times 10^{-9}$ and the respective $s$ values listed in Table 1; and the $\omega_v = 0.7/\tau_v$ value (↑) calculated with the same $K$. The upper dotted line is $G'(\omega)$ calculated without the $A_G\mu_G(t)$ term; the lower dotted line is calculated without both $A_G\mu_G(t)$ and $\mu_A(t)$.

In Figure 4, the frequency corresponding to the highest Rouse−Mooney normal mode, $\omega_v = 0.7/\tau_v$, is also indicated. One can see that at a temperature between 104.5 and 97 °C, $\omega_S$ becomes smaller than $\omega_v$, signaling the initiation of vitrification at the Rouse-segmental level, a prelude to the glass transition. This was pointed out in terms of the previously defined structural-relaxation time,[11] which reflected the similar effect of the glassy-relaxation process. In fact, as values of the previously defined $\tau_S$ at different temperatures are very close to the values based on the present definition (see Table 2 of ref 11), the discussion of the physical role of the structural relaxation in terms of $\tau_S$ defined by $G/R = 3$ remains essentially the same as in terms of the above-defined $\tau_S$, which has the additional advantage that, as shown below, its temperature dependence can be unambiguously compared with those of other dynamic quantities.

## 5. Comparison of the Temperature Dependences of Various Dynamic Quantities

For showing the chain dynamics in the polystyrene melt in perspective, the above analyses and discussions of the depolarized photon-correlation results and the creep compliance $J(t)$ can be put together by comparing the temperature dependences of the obtained dynamic quantities. The comparison, while confirming the validity of the physical picture in terms of which we have extensively analyzed the experimental results, summarizes the different physical roles as represented by these dynamic quantities.

Shown in Figure 5 are the $\langle\tau_c\rangle$ values obtained by Patterson;[13] the values of $\tau_v$ and $\tau_S$ as listed in Table 1; the temperature dependence of the viscosity corrected for changes in density and temperature, $\eta/\rho T$;[30,42] and the temperature dependence of the recoverable compliance $J_r(t)$ obtained by Plazek.[30,42] It is clear from the comparison that these dynamic quantities follow two distinctly different modes of temperature dependence: One, being steeper, is followed by $\tau_S$ and $J_r(t)$; the other one is followed by $\tau_v$, $\langle\tau_c\rangle$, and $\eta/\rho T$. In Figure 5, the unit scale on the vertical axis is for $\tau_v$ and $\tau_S$; the shown $\langle\tau_c\rangle$ points represent Patterson's values multiplied by 0.77;[46] and the $\eta/\rho T$ values and the shift factors in $J_r(t)$, as shown, have been individually multiplied by a proper factor so that they are superposed closely on the data points of $\tau_v$ and $\tau_S$, respectively. In the figure one

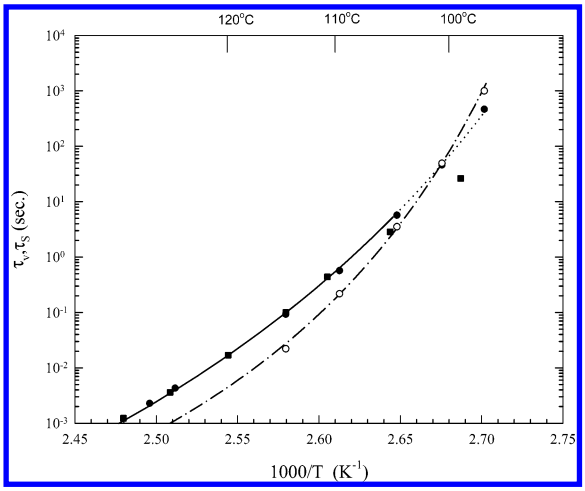


**Figure 5.** Comparison of $\tau_v$ (●), $0.77\langle\tau_c\rangle$ (■), and $\tau_S$ (○) as a function of temperature with the temperature dependence of $\eta/\rho T$ (—; the extended line below 104.5 °C is indicated by ···) and $J_r(t)$ (— · —); see the text.

can note that the temperature dependence of $\langle\tau_c\rangle$ above ~110 °C is parallel with and below ~110 °C becomes less steep than that of $\tau_v$ and $\eta/\rho T$. The reason for the divergence below ~110 °C will be explained below. In the steeper mode, the temperature dependence of $\tau_S$ and that of $J_r(t)$ are closely parallel with each other, representing the consistency between the two means of obtaining the temperature dependence of the creep compliance $J(t)$ in the small-compliance/short-time region: One is obtained from the analysis of the $J(t)$ results in terms of the combination of eqs 1, 4, and 5 of ref 11, while the other is obtained through empirical data reduction by Plazek.[30,42]

The temperature dependence of $\eta$ is calculated using the equation obtained by Plazek and O'Rourke[30,42] from the least-squares fitting to the data of sample A measured in the region ≥104.5 °C. This temperature dependence is in close agreement with those of other nearly monodisperse samples with a higher molecular weight to the lowest temperature—always higher than 104.5 °C—which is covered by the viscosity measurements of each individual sample.[30] As $\tau_v$, being calculated from $K$, reflects the temperature dependence of $K$ and the zero-shear viscosity is dominated by the dynamic processes whose temperature dependence is determined by $K$—the contribution from $A_G\mu_G(t)$ being in general negligibly small, the temperature dependence of $\tau_v$ and that of $\eta/\rho$T agree closely above 104.5 °C. With the guidance of the calculated $J(t)$ curves, the frictional factor $K$, which is used to calculate the $\tau_v$ value, can be determined at a temperature as low as the calorimetric $T_g$ (see Figure 1 of ref 11). As opposed to this, the viscosity of sample A could be determined only down to 104.5 °C.[30,42] However, below 104.5 °C, the extended $\eta/\rho T$ curve based on the same viscosity equation and the $\tau_v$ data points still have a good agreement. The agreement between the temperature dependences of $\tau_v$ and $\eta/\rho T$ as described above supports that the $K$ values listed in Table 1 have been correctly determined. To examine the comparison more closely, one may notice that when the temperature is close to $T_g$, the $A_G\mu_G(t)$ contribution to the zero-shear viscosity becomes slightly noticeable in the flow region of the $J(t)$ curve (see Figure 1 of ref 11)) because the $s$ value becomes large and, due to the molecular weight being not large, the terminal region of sample A is not far away in time. This effect may account for the slight tilt-up of the $\eta/\rho T$ curve in comparison to the $\tau_v$ points at temperatures close to 104.5 °C as vaguely suggested in Figure 5. As the effect is very small, the temperature dependence of $\tau_v$ and $\eta/\rho T$ is treated as the same in most discussions in this paper.

The steeper temperature dependence of $\tau_S$ (or $J_r(t)$) in comparison with that of $\tau_v$ (or $\eta/\rho T$) reflects the thermorheological complexity in $J(t)$. At slightly above 100 °C, $\tau_S$ crosses over $\tau_v$, signaling vitrification at the Rouse-segmental level. The crossing over is illustrated here in the real time scale as opposed to that shown in Figure 4 in a normalized time scale.

As pointed out above, the temperature dependence of $\langle\tau_c\rangle$ becomes less steep than that of $\tau_v$ below 110 °C, indicating surely that the dynamics observed by depolarized photon-correlation spectroscopy cannot be associated with the α- or glassy-relaxation process, whose temperature dependence is steeper than that of $\tau_v$. Furthermore, the glassy-relaxation process should very much involve strong interactions among segments belonging to different chains; in contrast, the effective optical anisotropy per monomer unit of polystyrene in bulk and in solution is the same indicating that the dynamics probed by depolarized photon-correlation spectroscopy does not involve correlation between segments belonging to different chains. Theoretically, one should not expect such an association either, as the photon-correlation measurement is based on the condition that the optical field obeys Gaussian statistics, requiring that the studied system be ergodic; as opposed to this, the emerging greater role of the glassy-relaxation process causes the loss of effective ergodicity as the temperature approaches $T_g$. While the parallel temperature dependence between $\langle\tau_c\rangle$ and $\tau_v$ (or $\eta/\rho T$) above 110 °C supports associating the dynamic process observed by depolarized photon-correlation spectroscopy with the motion of a Rouse segment, as discussed in Section 3; below ~110 °C, the gradual loss of ergodicity can have an effect on the dynamics as actually probed by depolarized photon-correlation spectroscopy. Especially, since the longest delay-time used in the photon-correlation measurement by Patterson *et al.*[13] is 1 s, the loss of effective ergodicty is a factor that cannot be ignored as $\tau_S$ exceeds 1 s at around 107 °C, and the actually measured $\langle\tau_c\rangle$ value exceeds 1 s. at just slightly below 110 °C. As shown by Pusey and van Megan,[47] if the intensity correlation function measured on a non-ergodic medium is analyzed by the method normally used for an ergodic medium, the *apparent* rate so obtained can be greater than the real rate by a large factor. The factor of course depends on how severe the loss of effective ergodicity is. Applying Pusey and van Megan's analysis here, the apparent $\langle\tau_c\rangle$ values obtained by Patterson et al. are expected to be smaller than the real values below 110 °C, where some loss of effective ergodicity begins to occur as explained above. This effect explains the weaker temperature dependence of $\langle\tau_c\rangle$ in comparison with that of $\eta/\rho T$ or $\tau_v$ below ~110 °C as shown in Figure 5.

## 6. Summary

Because of the large number of atoms and degrees of freedom in a chain molecule, a polymer is rich in its dynamics, with its relaxation-time distribution covering many decades. Different probing techniques are sensitive to different aspects of chain dynamics. To understand the chain dynamics in perspective, it is advisable to use different probing techniques to investigate the same (kind of) system; at the same time, it is desirable to relate the data obtained by the different techniques to one another through theoretical analyses and/or simulations. In this paper together with the companion paper, we show how the results of polystyrene obtained by the viscoelasticity and depolarized photon-correlation measurements are combined, giving a comprehensive picture of the dynamic processes in

the short-time region. The basic reason for the two techniques being particularly complementary to each other is that both probe the Brownian motion. From a preliminary analysis of experimental results, it was shown that the dynamics in polystyrene melt probed by depolarized photon-correlation spectroscopy should reflect the motion associated with a single Rouse segment. In the case of the concentrated polystyrene solution, the analysis benefiting from the Monte Carlo simulation has a high resolution confirming in a precise manner the interpretation of the depolarized photon-correlation results. By this it demonstrates that the size of a Rouse segment can be defined experimentally—in agreement with Inoue et al.[6−8,12]—and that its motion can be studied. That the temperature dependence of $\langle\tau_c\rangle$ is parallel with that of $\tau_v$ rather than that of $\tau_S$ is a logical consequence. As much discussed in the preceding paper,[11] using the description of the Brownian dynamic processes in $J(t)$ in terms of ERT as the reference frame in the analysis over the whole range, the glassy-relaxation process (namely, the α-relaxation) is characterized, showing that the thermorheological complexity in $J(t)$ as first observed by Plazek is closely related to the loss of ergodicity in approaching $T_g$. The temperature dependence of $\langle\tau_c\rangle$ becoming less steep than that of $\tau_v$ below 110 °C can be explained as due to the increasing loss of effective ergodicty when the temperature is lowered toward $T_g$.

In this study we have examined the Rouse-segmental motion in polystyrene as probed by depolarized photon-correlation spectroscopy in the light of the information obtained from the analysis of the $J(t)$ results as reported in the companion paper. It shows that the α-relaxation and the motion associated with a single Rouse segment are closely buried in the transition region—actually crossing each other just before reaching the calorimetric $T_g$. As a result, it is easy to mistake one for the other. This study has also proposed a way to define the α-relaxation time in polystyrene, with a clear physical meaning. Whether the same can be equally applied to other polymers remains to be seen.

**Acknowledgment.** This work is supported by the National Science Council (NSC 92-2113-M-009-027).

## Appendix

**Calculations of the Spectra of $G'(\omega)$, $G''(\omega)$, and tan $\delta$.** (Note: in this appendix, all the equations referred to are those in ref 11).

The spectra of storage and loss modulus and loss tangent of sample A as shown in Figures 3 and 4 are calculated by obtaining first its relaxation-time distributions at different temperatures as contained in the $G(t)$ curves shown in Figure 6 of ref 11. The $G(t)$ curves have been calculated from the combination of eqs 1, 4, 5, and 7 using the parameters $A_G$, $\beta$, and $s$ extracted from the analysis of the measured $J(t)$ curves. In all the calculations described below, the effect of the molecular weight distribution of the sample has been taken into account in the same way as explained in the analyses of $J(t)$[11] and calculations of $G(t)$.[4,16−18] To obtain the relaxation-time distribution of sample A, we can first consider two portions in eqs 1 and 4 separately: One is the part corresponding to ERT, namely, the portion without the $A_G\mu_G(t)$ term. The other is the $A_G\mu_G(t)$ term as contained in eq 4. In the former, all the theoretical forms of the relaxation processes and their relaxation times are known. Thus, for this portion a computer program can be constructed to accumulate the relaxation strengths of all the coupled or composite processes (arising from the product of two or three exponentially decaying functions) with relaxation times $\tau$ that fall in a small time interval, $\Delta \log \tau$, equally spaced in the log $\tau$ scale, giving the relaxation-time distribution with a resolution as high as one practically desires. On the other hand, the relaxation-time distribution of the $A_G\mu_G(t)$ term with $\mu_G(t)$ given by eq 5 can be calculated numerically.[38] For the present calculations, the resolution of 100 subdivisions per decade has been used throughout, which is more than ample. The total relaxation-time distribution can be formed from the distributions obtained for the two separate portions in accordance with the theoretical form as given by eqs 1 and 4. The obtained total relaxation-time distribution is first checked by calculating numerically the $G(t)$ curves for comparison with those calculated from eqs 1, 4, and 5 directly (i.e., those shown in Figure 6 of ref 11). Absolutely no discrepancy can be noticed between the two sets of $G(t)$ curves. With the relaxation-time distributions confirmed this way, the spectra of storage and loss modulus, and thus of loss tangent, can be calculated numerically in a straightforward manner. This approach of calculating $G'(\omega)$, $G''(\omega)$, and tan $\delta$ from $G(t)$—free of the approximation that is often involved in the conversion between the time and frequency domains[5]—is possible only because the theoretical form of $G(t)$ is known. As the measurement conditions—such as the use of the frictionless magnetic bearing and the control of temperature—in the creep experiment by Plazek are far more stringent than normally taken, the shown $G'(\omega)$, $G''(\omega)$, and tan $\delta$ spectra derived faithfully from the quantitative description of Plazek's $J(t)$ results should be much more reliable than ever obtained directly from a strain-controlled measurement.

## References and Notes

(1) Rouse, P. E., Jr. *J. Chem. Phys.* **1953**, *21*, 1271.
(2) Doi, M.; Edwards, S. F. *The Theory of Polymer Dynamics*; Oxford University Press: New York, 1986.
(3) Bird, R. B.; Curtiss, C. F.; Armstrong, R. C.; Hassager, O. *Dynamics of Polymeric Liquids, Vol. 2, Kinetic Theory*, 2nd ed.; Wiley: New York. 1987.
(4) Lin, Y.-H. *Polymer Viscoelasticity: Basics, Molecular Theories and Experiments*; World Scientific: Singapore. 2003.
(5) Ferry, J. D. *Viscoelastic Properties of Polymers*, 3rd ed.; Wiley: New York, 1980.
(6) Inoue, T.; Okamoto, H.; Osaki, K. *Macromolecules* **1991**, *24*, 5670.
(7) Inoue, T.; Hayashihara, H.; Okamoto, H.; Osaki, K. *J. Polym. Sci., Polym. Phys. Ed.* **1992**, *30*, 409.
(8) Inoue, T.; Osaki, K. *Macromolecules* **1996**, *29*, 1595.
(9) Lin, Y.-H. *J. Polym. Res.* **1994**, *1*, 51.
(10) Lin, Y.-H.; Lai, C. S. *Macromolecules* **1996**, *29*, 5200.
(11) Lin, Y.-H. *J Phys. Chem. B* **2005**, *109*, 17654.
(12) Inoue, T.; Uematsu, T.; Osaki, K. *Macromolecules* **2002**, *35*, 820.
(13) Patterson, G. D.; Lindsey, C. P.; Stevens, J. R. *J. Chem. Phys.* **1979**, *70*, 643.
(14) Lin, Y.-H. *Macromolecules* **1986**, *19*, 168.
(15) Lin, Y.-H.; Juang, J.-H. *Macromolecules* **1999**, *32*, 181.
(16) Lin, Y.-H. *Macromolecules* **1984**, *17*, 2846.
(17) Lin, Y.-H. *Macromolecules* **1986**, *19*, 159.
(18) Lin, Y.-H. *Macromolecules* **1987**, *20*, 885.
(19) Lin, Y.-H. *Macromolecules* **1991**, *24*, 5346.
(20) Doi, M.; Edwards, S. F. *J. Chem. Soc., Faraday Trans. 2* **1978**, *74*, 1789; **1978**, *74*, 1802.
(21) Lai, C. S.; Juang, J.-H.; Lin, Y.-H. *J. Chem. Phys.* **1999**, *110*, 9310.
(22) Lin, Y.-H.; Luo, Z.-H. *J. Chem. Phys.* **2000**, *112*, 7219.
(23) Lin, Y.-H. *J. Chin. Chem. Soc.* **2002**, *49*, 629.
(24) Mooney, M. *J. Polym. Sci.* **1959**, *34*, 599.
(25) Doi, M. *J. Polym. Sci., Polym. Phys. Ed.* **1980**, *18*, 1005.
(26) Mandel, L. *Prog. Opt.* **1963**, *2*, 181.
(27) Chu, B. *Laser Light Scattering: Basic Principles and Practice*; Academic Press: San Diego, 1991.
(28) Pecora, R., ed. *Dynamic Light Scattering: Application of Photon Correlation Spectroscopy*; Plenum Press: New York, 1985.
(29) Berne, B. J.; Pecora, R. *Dynamic Light Scattering*; Wiley: New York, 1976.
(30) Plazek, D. J.; O'Rourke, V. M. *J. Polym. Sci. Part A-2*: *Polym. Phys.* **1971**, *9*, 209.
(31) Lindsey, C. P.; Patterson, G. D.; Stevens, J. R. *J. Polym. Sci., Part B: Polym. Phys.* **1979**, *17*, 1547.

(32) Ballard, D. G. H.; Rayer, M. G.; Schelten, J. *Polymer* **1976**, *17*, 349.

(33) Norisuye, T.; Fujita, H. *Polym. J.* **1982**, *14*, 143.

(34) Fischer, E. W.; Dettenmaier, M. *J. Non-Cryst. Solids* **1978**, *31*, 181.

(35) Ehrenburg, E. G.; Piskareva, E. P.; Poddubnyi, I. Y. A. *J. Polym. Sci., Polym. Symp.* **1973**, *No. 42*, 1021.

(36) Alms, G. R.; Bauer, D. R.; Brauman, J. I.; Pecora, R. *J. Chem. Phys.* **1973**, *59*, 5310.

(37) It has been shown by the Monte Carlo simulation in ref 22 that for the mean square length of a Rouse segment $\langle \mathbf{b}^2 \rangle$ set at 100, $\langle |\mathbf{b}| \rangle = 9.23 \approx \langle \mathbf{b}^2 \rangle^{1/2}$. On this basis, the Rouse segment and the Kuhn segment can be treated as basically equivalent to each other. In ref 8, Inoue and Osaki have given the sizes of the Rouse segment and the Kuhn segment for various polymers, showing that they are basically the same.

(38) Lindsey, C. P.; Patterson, G. D. *J. Chem. Phys.* **1980**, *73*, 3348.

(39) In ref 12, the *m* value is calculated from the rubbery modulus at high-frequency limit extracted from analyzing the dynamic mechanical and birefringence results. As opposed to Inoue's *m* value being calculated from a *static* quantity, the depolarized photon-correlation and viscosity data, as correlated to obtain *m*, are *dynami*c quantities.

(40) Hopkins, I. L.; Hamming, R. W. *J. Appl. Phys.* **1957**, *28*, 906; **1958**, *29*, 742.

(41) Tschoegl, N. W. *The Phenomenological Theory of Linear Viscoelastic Behavior*; Springer-Verlag: Berlin, 1989.

(42) Plazek, D. J. *J. Phys. Chem.* **1965**, *69*, 3480.

(43) Plazek, D. J. *J. Polym. Sci. Part A-2: Polym. Phys.* **1968**, *6*, 621.

(44) McCrum, N. G.; Read, B. E.; Williams, G. *Anelastic and Dielectric Effects in Polymeric Solids*; Dover: Mineola, NY, 1991.

(45) Such a small shift between $\omega$ and $1/t$ is also indicated on page 323 of ref 5.

(46) Note: Several factors affect the ratio between $\tau_v$ and $\langle \tau_c \rangle$: As given by eq 8 of ref 11, the ratio of $K'$ to $K$ used in calculating $\tau_v$ depends on the molecular weight of the sample. Here, $\tau_v$ is for sample A whose $M_w$ value is $4.69 \times 10^4$ ($K'/K = 1.61$), while the $\langle \tau_c \rangle$ values obtained by Patterson et al.[13] are for a sample whose molecular weight should be in the region where its $K'/K$ ratio is at the plateau value 3.3. Experimentally $\langle \tau_c \rangle$ represents the average relaxation time of a dynamic process whose broad relaxation-time distribution (corresponding to $\beta = 0.4$) may also modify its absolute magnitude.

(47) Pusey, P. N.; van Megan, W. *Physica A* **1989**, *157*, 705.